CellPress
OPEN ACCESS

Neuron

Perspective

Rhythmic attentional scanning

Pascal Fries[1,2,*]
[1]Ernst Strüngmann Institute (ESI) for Neuroscience in Cooperation with Max Planck Society, 60528 Frankfurt, Germany
[2]Donders Institute for Brain, Cognition and Behaviour, Radboud University Nijmegen, 6525 EN Nijmegen, the Netherlands
*Correspondence: pascal.fries@esi-frankfurt.de
https://doi.org/10.1016/j.neuron.2023.02.015

SUMMARY

Sensory processing, short-term memory, and decision-making often deal with multiple items, or options, simultaneously. I review evidence suggesting that the brain handles such multiple items by "rhythmic attentional scanning (RAS)": each item is processed in a separate cycle of the theta rhythm, involving several gamma cycles, to reach an internally consistent representation in the form of a gamma-synchronized neuronal group. Within each theta cycle, items that are extended in representational space are scanned by traveling waves. Such scanning might go across small numbers of simple items linked into a chunk.

INTRODUCTION

In many brain areas of many species, neuronal activity shows theta rhythmicity and theta-rhythmic modulation of gamma rhythmicity.[1–4] I propose that similarities in the spatiotemporal organization of these theta-gamma rhythms often reflect a common functional role, namely, the "rhythmic attentional scanning (RAS)" of the respective brain areas and/or of their representational spaces, defined in the visual cortex by visual (feature) space and in hippocampus by an animal's location, for example. In these representational spaces, there are often theta-rhythmically reoccurring traveling waves, likely corresponding to waves of enhanced neuronal excitability, which might serve as attentional scans. These scans often start at the representation of the recent position of the body, of the fovea, or of the attentional focus. Within one theta cycle, a behaviorally relevant segment of the respective space is scanned, e.g., a segment of an upcoming path or a visual object. Different segments are scanned in separate theta cycles. Theta phase modulates local excitability and thereby gamma activity and long-range gamma synchronization. In sensory cortices, these gamma processes reflect attentional selection, and this might generalize to other brain areas. Thereby, theta-rhythmic waves of gamma might implement theta-rhythmic attentional scanning.

I use the term "scanning" to refer to the smooth propagation of attention, in the form of a traveling excitability wave, within a single theta cycle; I use the term "sampling" to refer to the sequential selection of discrete stimuli for preferential processing, across subsequent theta cycles. If multiple stimuli are simultaneously present, yet one is sampled in disproportionally many theta cycles, this realizes selective attention to the respective stimulus.

ATTENTION AS ENHANCED RHYTHMIC-SAMPLING PROBABILITY

Attention has been prominently conceptualized in a framework that stems from cognitive psychology[5] (but see Anderson[6]), which assumes that attention is at the attended location for an extended period of time. However, extended focusing on a single location might not be optimal under natural conditions, when the visual system is typically faced with several stimuli simultaneously. The RAS hypothesis proposes that multiple simultaneously present items are selected sequentially, item by item (Figure 1A). A given item is selected for one theta cycle. Within a theta cycle, multiple gamma cycles are involved in the routing of the selected stimulus to higher areas for full processing. If the selected stimulus is extended, its representation can be scanned by a traveling wave within a theta cycle. Separate theta cycles sample any number of simultaneously present stimuli. If one or a subset of those stimuli is behaviorally relevant, they are sampled with higher probability. This enhanced sampling probability corresponds to the notion of attention as a cognitive function.[7] The individual sampling event can be considered a notion of attention as a neuronal process. I will review empirical evidence about these attentional processes from the visual system, the hippocampus, and the prefrontal cortex (PFC) to revise the concept of attention as a cognitive function, thereby proceeding "from inside out[8]."

RHYTHMIC SCANNING IN THE VISUAL SYSTEM

Neuronal mechanisms of selective visual attention have been captured in models containing the concept of convergence. Anatomical projections from a lower to a higher visual area typically show convergence, such that smaller receptive fields in the lower area are combined to form larger receptive fields with more complex stimulus selectivities.[9,10] Those larger receptive fields often contain multiple objects, in the following referred to as (visual) stimuli. Two stimuli inside the receptive field of one higher-level visual neuron lead to two competing sets of synaptic inputs to this neuron.[11] When attention is directed to one of those stimuli, the resulting attentional effects on this neuron's firing rates can be modeled as an enhanced gain of the synapses conveying the attended stimulus.[12–14] This selective gain enhancement might be implemented by selective neuronal gamma-band (40–90 Hz) synchronization in at least two ways. One way is an

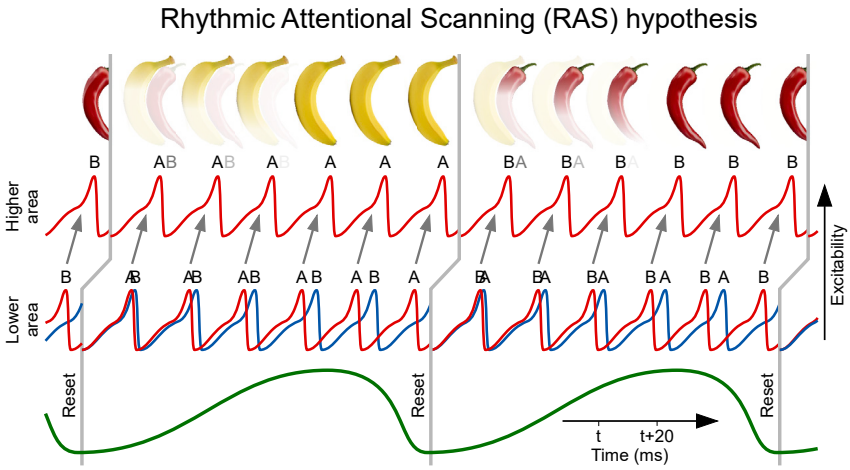

Figure 1. Rhythmic attentional scanning (RAS)

Rhythmic attentional scanning (RAS) hypothesis: two stimuli, A and B, activate two corresponding neuronal groups, A and B, in a lower visual area. Those groups have convergent projections onto neurons in a higher visual area. In the neuronal groups of the lower area, the two stimuli induce two gamma rhythms, illustrated as red and blue excitability time courses. A theta rhythm, illustrated on the bottom by a green line, rhythmically resets the phase of both gamma rhythms, indicated by vertical gray lines (displaced to the right between lower and higher area to reflect inter-areal delay). After each reset, one of the lower-area gamma rhythms wins the competition to entrain the gamma rhythm in the higher area, whereas the other lower-area gamma rhythm loses. The competition might be influenced by the frequencies of the two lower-area gamma rhythms: in each theta cycle, one of those rhythms is slightly faster; after each theta-rhythmic reset, the faster gamma provides input to the higher visual area that arrives slightly before input from the slower gamma; the earlier input can drive the higher area neurons and trigger inhibition, which shuts out the later input. Yet, this frequency-dependent competition is not essential for RAS; the core point is that in each theta cycle, one gamma rhythm, corresponding to one stimulus, entrains the higher area and thereby provides selective routing of that stimulus to the higher area. While the RAS hypothesis is illustrated for two stimuli, it can apply to more. Note that it does not need to apply to all stimuli that are contained in the entire visual field, but it merely needs to apply to the number of stimuli that actually compete with each other due to convergence onto a postsynaptic target neuron.

attentional enhancement of feedforward coincidence detection. Gamma-band synchronization of neurons representing the attended stimulus renders the corresponding synaptic inputs to a postsynaptic neuron coincident in time. Coincident synaptic inputs benefit from effective postsynaptic summation, also termed coincidence detection.[15,16] Indeed, neuronal gamma-band synchronization in macaque V4 is enhanced by attention to the respective stimulus.[17–19] Furthermore, trial-by-trial fluctuations of this local gamma-band synchronization predict trial-by-trial fluctuation of RTs, i.e., of behavioral benefits of attention.[20] Another way in which gamma might subserve selective gain enhancement has been referred to as communication through coherence (CTC): if the gamma-rhythmic synchronization of neurons representing the attended stimulus entrains postsynaptic neurons, this can time the respective synaptic inputs to moments of high postsynaptic excitability and thereby effectively enhance synaptic input gain[21–24] (Figure 1A). Indeed, neuronal gamma-band synchronization between macaque V1 and V4 neurons with overlapping RFs is strongly enhanced by attention to the stimulus represented by the respective V1 neurons.[25,26] Furthermore, trial-by-trial fluctuations of this inter-areal gamma-band synchronization predict trial-by-trial fluctuations of RTs, and this inter-areal gamma synchronization occurs at the optimal phase relation for transmission of sensory inputs to motor responses.[27]

Both mechanisms, feedforward coincidence detection and CTC, enhance synaptic gain selectively for the synapses conveying the attended stimulus. The "attended-stimulus synapses" arriving at a given postsynaptic neuron constitute a subset of all its inputs. The complete set of a postsynaptic neuron's inputs can be activated in almost infinitely many combinatorial ways by one or multiple stimuli in its receptive field. Each stimulus corresponds to a subset of inputs, and the segmentation of this subset, and thereby their binding, is a form of the binding problem. The segmentation of the "attended-stimulus inputs" and the increase in their gain can both be implemented by selective inter-areal gamma-band synchronization.[28] Gamma synchronization within a theta cycle thus implements the attentional sampling of one stimulus from all stimuli competing for influence on the postsynaptic neuron. Note that the dynamic increase in synaptic gain through inter-areal synchronization implements transient synaptic potentiation in vertical assemblies, as proposed in "the searchlight hypothesis."[29]

When attention is engaged with one stimulus, processing resources—particularly in higher visual areas—are exploited selectively to analyze the attended stimulus. Yet, there is a trade-off between exploitation and exploration. As long as processing resources are devoted to one stimulus, other stimuli are ignored. Therefore, after the analysis of one stimulus has reached a sufficient level, the visual system might explore other stimuli. Much of the analysis of one stimulus is accomplished within approximately 120–150 ms.[30,31] If the visual system were to explore another stimulus every 120–150 ms, this would constitute a 7–8 Hz theta rhythm. Intriguingly, much evidence now suggests that indeed, attention samples the visual world at a theta rhythm.

As reviewed above, attentional stimulus selection is implemented by gamma-band synchronization. Gamma-band synchronization can occur in the absence of theta, e.g., during non-REM sleep,[32] yet during the awake and attentive state is often modulated theta rhythmically.[1–4,25] If gamma implements attention and is modulated theta rhythmically, it suggests that attentional stimulus selection occurs theta rhythmically. Indeed, the theta rhythm might govern overt attentional exploration and also memory formation.[33] When primates can freely explore scenes with their eyes, the location of attention is typically at the fovea, and shifts in attention are related to saccadic shifts in fixation position. Thereby, saccades are overt expressions of shifts in attention. Covert shifts of attention during fixation are reflected in microsaccades.[34] When human subjects explore visual scenes, the distribution of inter-saccadic intervals shows a characteristic peak (Figure 2A) that is consistent with a ~6–8 Hz rhythmicity.[35] Furthermore, when human subjects saccade from

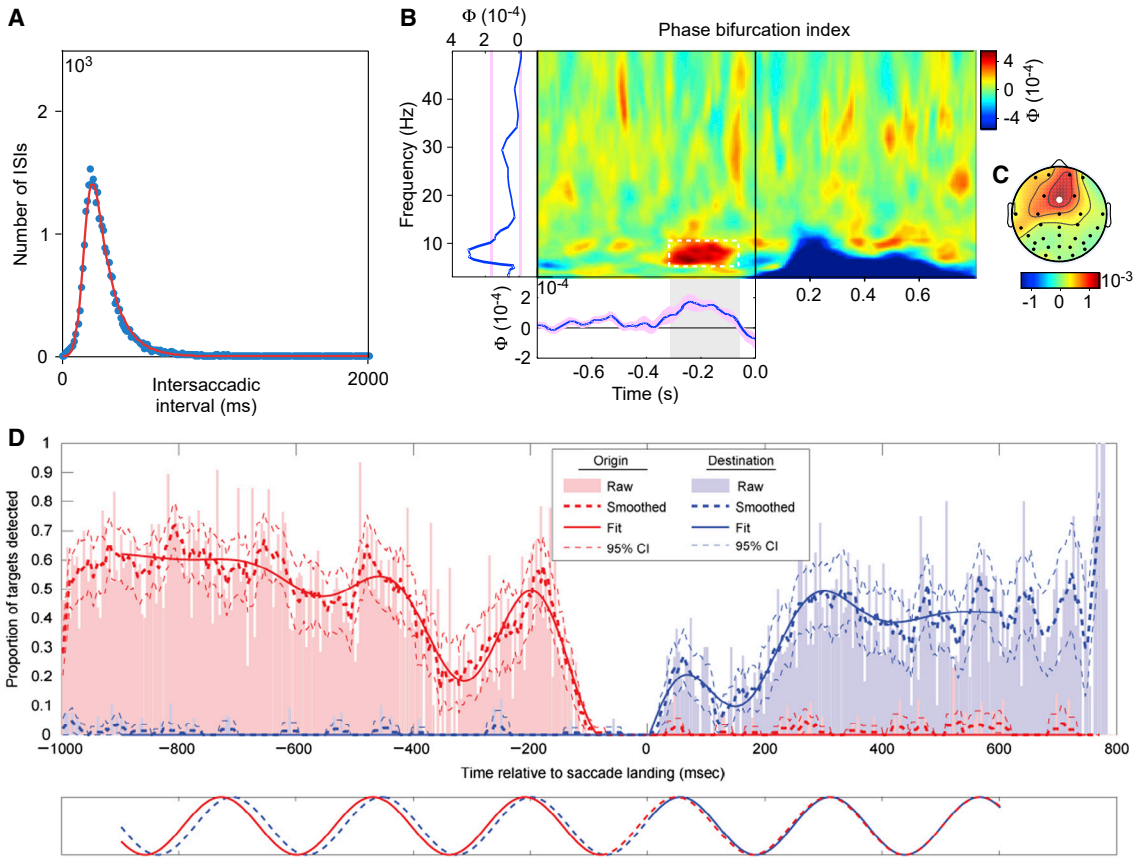

Figure 2. Theta rhythmicity in saccade behavior and detection performance

(A) Distribution of intersaccadic intervals for regular saccades of human subjects exploring natural scenes. Adapted and modified from Otero-Millan et al.[35]

(B) Phase bifurcation index as a function of time relative to stimulus onset (x axis) and frequency (y axis). Positive values indicate that EEG phase distributions are locked to different phase angles for hits and misses (e.g., in the pre-stimulus time range), while negative values indicate that only one condition is phase locked (e.g., phase locking exclusively for hits in the ERP time range). Left marginal, average over time; bottom marginal, average over 6–10 Hz.

(C) Topography of phase bifurcation index averaged over 6 to 10 Hz and −300 to −50 ms preceding stimulus onset. (B) and (C) are adapted and modified from Busch et al.[37] (copyright 2009 Society for Neuroscience).

(D) Detection performance as a function of time relative to saccade landing. Saccades go from an origin grating to a destination grating, and performance is measured and quantified independently for the origin (red) and destination (blue). Adapted and modified from Hogendoorn.[36]

one grating stimulus to another, their ability to report a threshold-level change in any one of those stimuli, a measure of attention, is modulated at ~4 Hz (Figure 2D).[36] This ~4 Hz rhythm might reflect a sub-harmonic of an ~8 Hz attentional sampling rhythm, distributed across the two stimuli, as discussed below. The ~4 Hz modulation is aligned to the saccade-landing time, and it affects attention both to the second stimulus after the saccade and the first stimulus before the saccade. In fact, when the two stimuli's attentional benefits are independently quantified, the theta-rhythmic components have virtually the same frequency and phase (blue and red sine waves in Figure 2D, bottom panel). This suggests that "saccades are executed as part of an ongoing attentional rhythm, with the eyes in flight during the troughs of the attentional wave.[36]" Thus, attention, saccades, and their neuronal mechanisms are linked at a theta rhythm, such that an attribution of cause or consequence to one of them might not be possible.[8]

Other studies have demonstrated that enhanced detection performance, one of the hallmarks of attention, is modulated with a brain rhythm of ~7 Hz.[37] In one study, human subjects fixated centrally and monitored a peripheral location for a brief and weak visual probe stimulus. The electroencephalogram (EEG) was measured, and the analysis tested whether the EEG before probe onset predicted detection performance. The detection performance could indeed be partly predicted by the phase of the 7.3 Hz EEG component primarily over frontal brain regions (Figures 2B and 2C). This result suggests that a frontal theta rhythm modulates the capacity to process and/or report about the monitored visual field location.

This theta-rhythmic modulation of visual processing could be global to the entire visual field, or it could reflect an attentional sampling process. A crucial component of attention is the prioritization of one location or stimulus over other locations or stimuli. Thus, if the 7 Hz modulation of detection performance at one peripheral location reflects attentional sampling, then momentary attentional biasing toward that location should coincide with attentional biasing away from other locations. Such moment-to-moment biases of attention have actually been

suggested by electrophysiological measurements, which can record previously established neuronal signs of attention with millisecond resolution. As mentioned above, previous studies established that attention enhances visually induced gamma-band activity in intermediate and higher visual areas.[17,19,38] Gamma-band synchronization in V4 is partially predictive of behavioral RTs, a central benefit of selective attention.[20] When, in a given trial, the RT to the behaviorally relevant stimulus change is particularly short, this is preceded by (1) particularly strong gamma-band synchronization among the V4 neurons representing this stimulus and (2) particularly weak gamma-band synchronization among the V4 neurons representing a distracter stimulus.[20] Particularly short RTs likely result from momentarily focused selective attention, and the results show that this entails both enhanced processing of the attended and reduced processing of the unattended stimulus.

Gamma-band synchronization between macaque V1 and V4 indexes attention to the stimulus activating the V1 recording site (Figure 3A), and this V1–V4 gamma synchronization is modulated theta rhythmically (Figure 3B).[25] A later MEG study with human subjects investigated whether such theta-rhythmic attentional biasing of gamma is predictive of behavior. Human subjects distributed attention to two stimuli in the left and right visual hemifield (Figure 3C). The two stimuli induced sustained gamma-band activity in the respective contralateral visual cortex. Any moment-to-moment attentional bias to one of the two stimuli should be reflected in the difference between the respective gamma-band responses, referred to as lateralized gamma activity (LGA) (Figure 3C). The LGA in higher visual areas indeed predicted attentional performance, with opposite 4 Hz phases of LGA fluctuations predicting high detection accuracy in the left versus right hemifield (Figures 3D–3F). This is again consistent with an 8 Hz attentional sampling, alternating between the two stimuli.

Another electrophysiological real-time metric of the focus of attention are the firing rates in primate inferotemporal (IT) cortex. IT cortex is close to the top of the hierarchy of visual areas. A given IT neuron typically has a very large RF and exhibits clear stimulus preferences. A preferred stimulus drives the neuron to high firing rates, whereas a nonpreferred stimulus drives the neuron to low firing rates. When a preferred and a nonpreferred stimulus are presented simultaneously inside the RF, and when attention is directed to one of them, the neuron's response is dominated by the attended stimulus.[40,41] Therefore, the momentary IT neuron firing rate can be used as an index of the momentary focus of selective attention. It is also known that selective attention is automatically drawn to a new stimulus.[42] In a seminal study on IT neuronal firing rates, one stimulus was first presented for 600 ms and remained on the screen after a second, new stimulus was added.[43] When the neuron's nonpreferred stimulus was added to a preferred stimulus, the firing rate showed a trough followed by a peak followed by a trough and so on for a few cycles; when the neuron's preferred stimulus was added to a nonpreferred stimulus, the firing rate showed a peak followed by a trough followed by a peak and so on for a few cycles (Figure 4A). These sequences suggest that the onset of a new stimulus caused the attentional selection of that new stimulus, followed by an alternating attentional selection of the two stimuli. The resulting firing-rate oscillation showed peaks at ~5 Hz (Figure 4B), suggesting attentional selection of the preferred stimulus at 5 Hz and an overall attentional sampling rhythm of ~10 Hz.

Thus, the onset of a new stimulus essentially resets attentional sampling and thereby reveals the rhythmicity of attentional sampling. If attention indeed alternates between the two stimuli, this should result in alternating attentional improvements in behavioral performance on those two stimuli. This prediction was tested in a subsequent psychophysical study in human subjects.[44] Subjects distributed attention to two peripheral stimuli at equal eccentricities to the left and right of the fixation point. In each trial, one of the stimuli underwent a hard-to-detect change at an unpredictable moment in time. Detection performance for this change served as a behavioral index of attention to the respective stimulus at the respective time. In each trial, a task-irrelevant flash was presented around one of the two stimuli to automatically draw attention to the respective side. As an unavoidable side effect, the flash caused some masking, with the corresponding transient reduction in detection performance. When this masking was over, and when the flash had been presented around the stimulus in the right hemifield, subsequent detection performance fluctuated at ~4 Hz (Figures 4C and 4D). Crucially, detection performance for the stimulus in the other hemifield fluctuated at essentially the same frequency, yet at approximately opposite phase (Figure 4D, inset). These results are consistent with an 8 Hz attentional sampling, which samples the two stimuli in alternation. Note that when the flash occurred in the left visual hemifield, detection performances for the two stimuli also showed rhythmic modulation, yet at different frequencies, and this might be related to the fact that the corresponding right temporal parietal areas are involved in attentional reorienting generally, not just toward one side.

One particularly elegant study used a sophisticated paradigm to measure the temporal frequency of attentional sampling, when attention was devoted to a single stimulus or distributed over two or three stimuli.[45] When attention was devoted to a single stimulus, this stimulus was sampled at ~7 Hz. When attention was distributed over two stimuli, the attentional sampling frequency per stimulus dropped to ~7 Hz divided by 2. And when attention was distributed over three stimuli, the attentional sampling frequency per stimulus dropped to ~7 Hz divided by 3. Thus, also these data are consistent with an attentional sampling routine that operates at ~7 Hz and samples separate stimuli sequentially.

Another study provided seminal insight into attentional sampling, when it either samples two locations on two different stimuli or alternatively two locations on two different positions on the same stimulus.[46] In a given trial, either two vertical bars were placed right and left of the fixation point, or two horizontal bars were placed above and below the fixation point, each time such that all four ends of the two bars were at equal eccentricities from the fixation point. In a given trial, a flash occurred around one end of one of the bars, automatically drawing attention to this location and cueing this end as the behaviorally most relevant one (Figure 5A). Subsequently, a hard-to-detect change occurred either on the cued bar at the cued end (75% of trials), on the cued bar at the uncued end (12.5%), or on the uncued

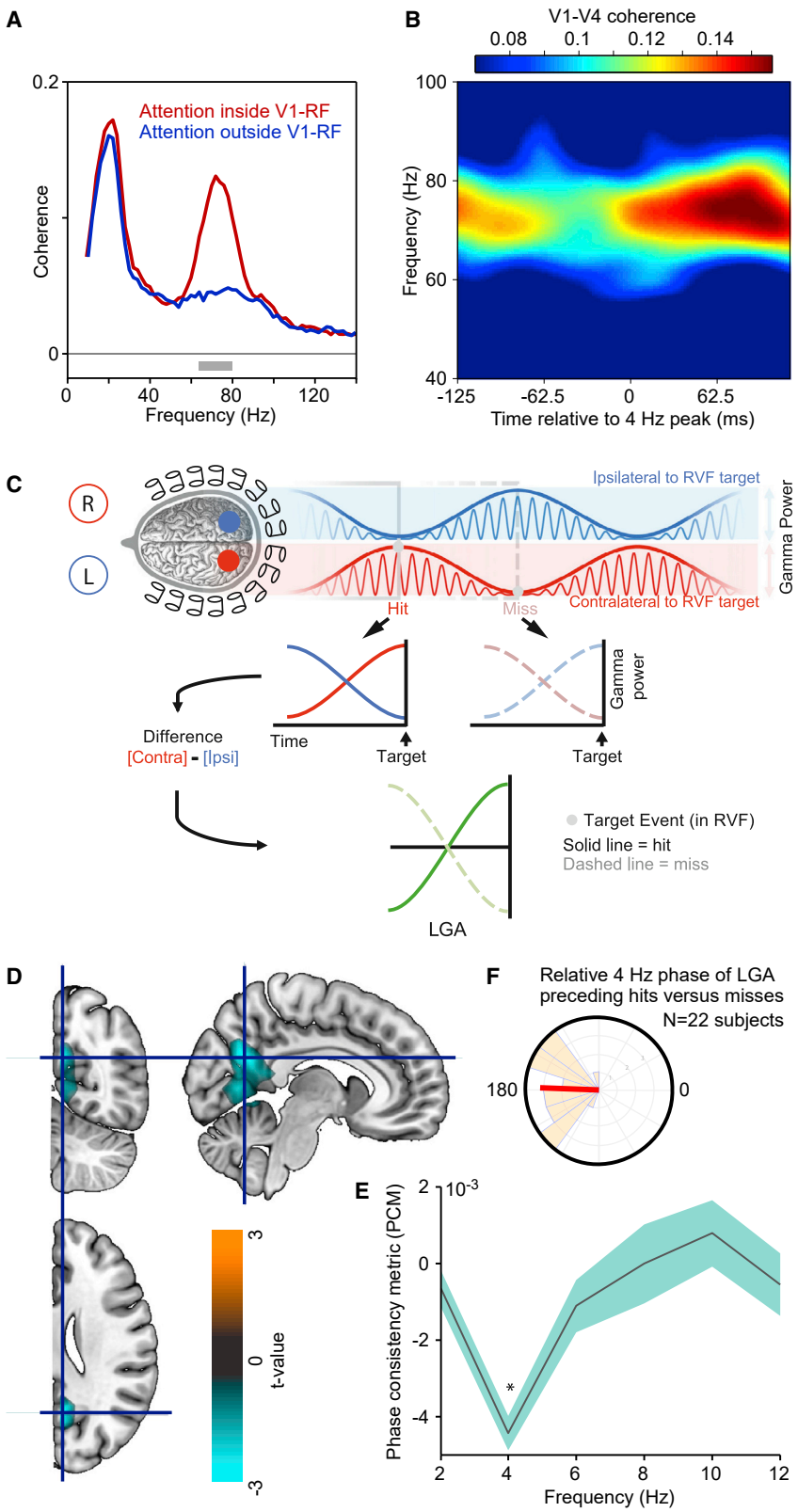

Figure 3. Theta-rhythmic attentional sampling without an attentional reset event

(A) Spectral coherence between neuronal activities recorded in areas V1 and V4 of a macaque, when selective attention is inside (red) or outside (blue) the V1-RF. The V1 site is activated by one of two simultaneously presented grating stimuli, which both activate the V4 site approximately equally.

(B) Same analysis as the red line in (A), i.e., V1-V4 coherence during attention inside V1-RF, yet here analyzed as a function of the time relative to 4 Hz peaks (x axis), and color-coded as shown by the color bar on the top. (A) and (B) are adapted and modified from Bosman et al.[25]

(C–F) (C) Illustration of a test for rhythmic attentional sampling in human subjects with MEG, leading to the results in (D)–(F). Two visual stimuli in the two visual hemifields induce two gamma rhythms in the respective opposite hemispheres, whose amplitude envelopes (thick blue and red lines) are modulated at theta, in anti-phase between the hemispheres/stimuli. The difference between those envelopes, the lateralized gamma-band activity (LGA; green lines), eliminates unspecific fluctuations and isolates momentary attentional biases to one versus the other stimulus. The LGA can be analyzed for the time period preceding stimulus changes that were detected (hit, solid green line) or remained undetected (misses, dashed green line).

(D) The experimentally obtained LGA was spectrally analyzed, and significant anti-phase relationship (phase consistency metric, PCM) preceding hits versus misses was quantified at the MEG source level. Across sources and frequencies (2–20 Hz), there was one significant cluster of adjacent sources spanning calcarine sulcus, lingual gyrus, and precuneus gyrus, whose t values (two-sided t test across subjects) are shown here as color code.

(E) PCM averaged over the sources in the cluster from (D), as a function of frequency. The shaded region indicates the mean ± 1 SEM across subjects. The anti-phase relationship existed specifically at 4 Hz.

(F) Distribution of relative 4 Hz phase of LGA preceding hits versus misses, across the 22 subjects. (C)–(F) are adapted and modified from Landau et al.[39]

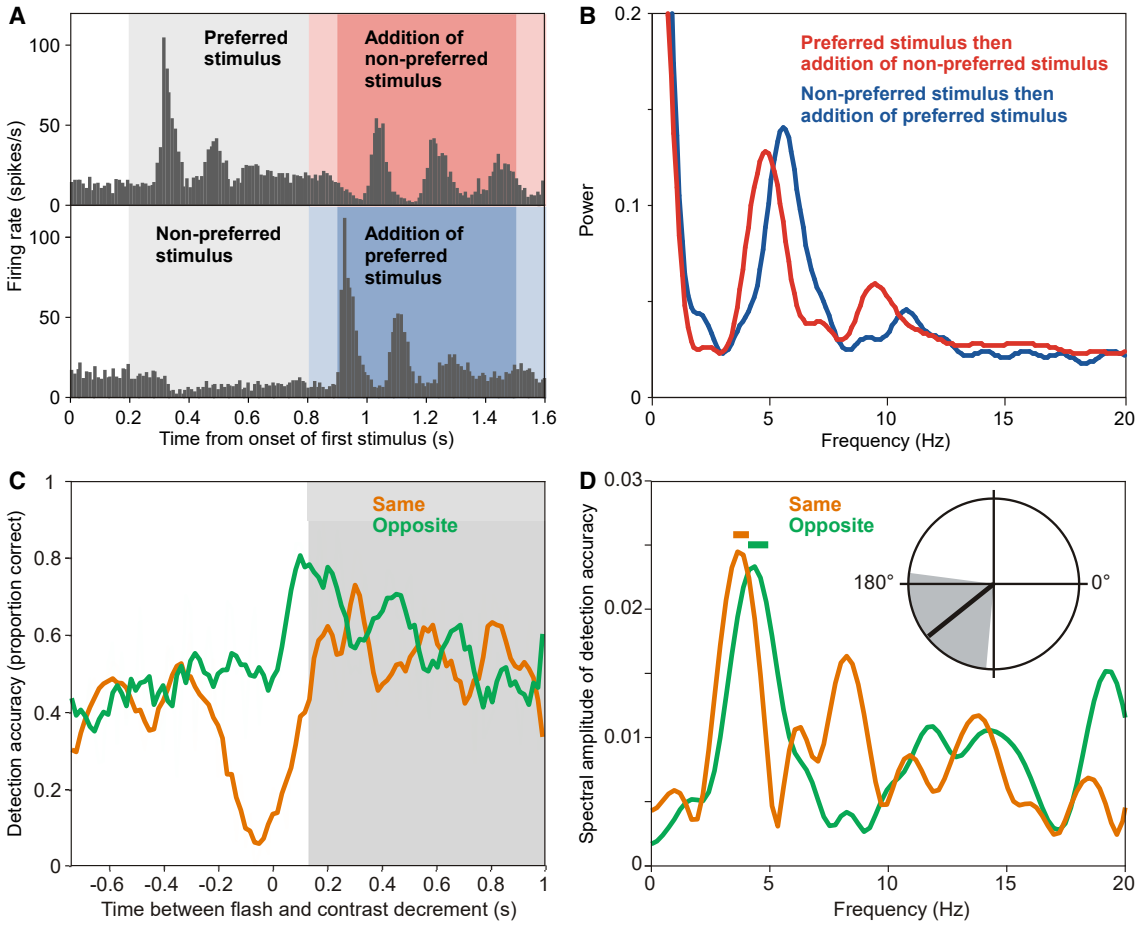

Figure 4. Theta-rhythmic attentional sampling after an attentional reset event

(A and B) (A) Firing rate of an example neuron recorded from inferotemporal (IT) cortex of an awake macaque during the indicated stimulation conditions. First, either a preferred or a nonpreferred stimulus was presented for 0.6 s. Subsequently, a nonpreferred or a preferred stimulus was added (reset event) in the red (or blue) shaded time period. The slightly darker shading indicates the time period for which autocorrelograms (ACGs) and power spectra of those ACGs, as shown in (B), were computed.

(B) Power spectra of the indicated conditions, for the periods shown in darker red (or blue) shading in (A). (A) and (B) are adapted and modified from Rollenhagen and Olson.[43]

(C) Detection accuracy (smoothed for illustration) as a function of time between a flash (reset event) in the right visual hemifield and a probe (contrast decrement) in the same (orange) or opposite (green) hemifield as the flash.

(D) Amplitude spectra of the non-smoothed detection accuracy, using the same color-coding as in (C) and for the time period indicated by the gray shading in (C). Horizontal bars indicate frequencies with significant modulation ($p < 0.05$, compared with time-shuffled accuracy time courses, Bonferroni corrected across frequencies). Polar plot shows mean phase relation between the theta rhythms (3.6–4.8 Hz) in the two conditions. (C) and (D) adapted and modified from Landau and Fries.[44]

bar at the end that had a distance of one bar length from the cued location (12.5%) (Figure 5B). After the cue-flash had occurred, change detection performance fluctuated rhythmically and with a very interesting pattern of phase relations (Figures 5C and 5D). Detection performance at the two uncued locations on the two bars fluctuated at 4 Hz and approximately in anti-phase (Figure 5E). This is again consistent with an 8 Hz attentional sampling, alternating between the two bars. Most intriguingly, detection performance at the cued and the uncued location on the same bar fluctuated at 8 Hz and with a 90°, or 31 ms, lag for the uncued location (Figure 5F). This suggests that within a given stimulus, a theta-rhythmic attentional sampling routine, potentially implemented by a theta-rhythmic neuronal excitability wave, might start at the attended location and scan across the rest of the stimulus. Evidence for such an implementation of theta-rhythmic attentional scanning is difficult to obtain with psychophysical experiments. Yet, physiological studies do provide evidence indicating that such scanning might actually occur.

One study used voltage sensitive dyes to record neuronal depolarization from substantial portions of the surface of areas V1 and V2 of awake macaque monkeys.[47] When a small visual stimulus was presented, it first evoked neuronal depolarization in the retinotopically corresponding part of area V1. From there, depolarization propagated across the cortical surface in the form of a traveling wave (Figure 6A). At the same time, a similar traveling wave propagated across the surface of area V2, and the two traveling waves maintained a precise phase relation. As neuronal

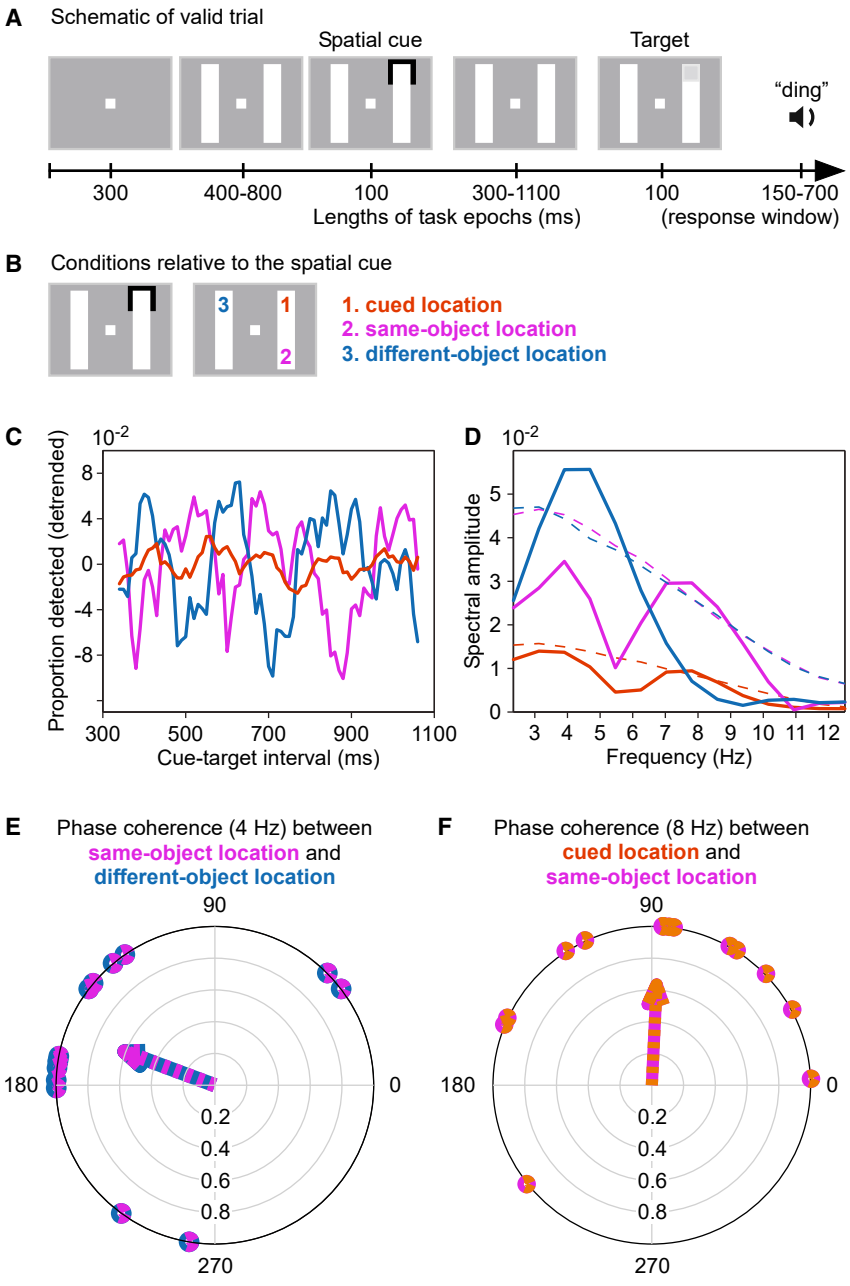

Figure 5. Evidence consistent with rhythmic attentional scanning within a stimulus

(A–F) (A) Trial structure of a psychophysical experiment to investigate rhythmic sampling within and between stimuli. During continued fixation, two bars are shown, and one end of one bar is cued. The cue acts as attentional reset event. At a variable time after the cue, the target appears at the cued location, illustrated here (valid trial), or at one of two alternative positions shown in (B).

(B) The bars can be arranged vertically, as shown here, or horizontally. The cue-flash can appear at either one of the ends of either one of the bars. If the cue-flash appears as indicated on the left, the possible target locations are as indicated on the right, with their respective labels and color codes, used in (C)–(F).

(C) Target detection performance as a function of cue-target interval, separately for the three conditions, as color-coded in (B).

(D) Power spectra (solid lines) and their corresponding significance thresholds (dashed lines). Note that power spectra of the cued location (orange) cannot be directly compared with the other power spectra, because this location was probed in far more trials.

(E) Each dot on the outer circle reflects, for one participant, the phase relation at 4 Hz between their detection performances at the same-object versus different-object location. The arrow points toward the average phase relation.

(F) Same as (E), but for the phase relation at 8 Hz between detection performances at the cued location versus the same-object location. (A)–(F) are adapted and modified from Fiebelkorn et al.[46]

depolarization is closely related to neuronal excitability, these results demonstrate that a stimulus evokes waves of neuronal excitability that smoothly propagate across the representation of visual space and might serve as a mechanism for attentional scans. Thus, in the abovementioned psychophysical study with a flash around the end of one of two bars, this flash might well have evoked a traveling wave of excitability and thereby a traveling wave of attention. Because the flash served as an attentional cue, this wave started from the cued location on the cued bar. If we assume that the wave traveled preferentially along the contiguous cortical representation of the bar, this could explain why high detection performance at the cued location was followed 31 ms later by high detection performance at the uncued location on the cued bar.

During natural viewing, primates consistently make saccades or microsaccades, likely accompanied by top-down input reflecting the movement-related sensory prediction.[8] Furthermore, the movement of the eyes generates a transient motion of the projection of the visual field onto the retina. Such a transient, potentially in concert with the corresponding top-down input, might conceivably lead to a similar traveling wave as described above in response to a visual flash stimulus. Indeed, such post-saccadic waves were discovered in recordings of macaque area V4.[48] Macaques performed saccades of 5–20 deg length, while neuronal activity was recorded from 96 sites representing retinal eccentricities ranging from 3 to 30 degrees. Intriguingly, saccades triggered traveling waves that started after the saccade and propagated from the representation of the fovea or parafovea to the representation of the visual periphery (Figure 6B). These waves were observed in the local field potential (LFP) filtered at 20–40 Hz, yet were triggered by saccades. Saccades, as mentioned above, occur at intervals consistent with a theta rhythm and aligned to theta-rhythmic attentional modulation. Thus, theta-rhythmic saccades might set off theta-rhythmic attentional scans. Those scans might

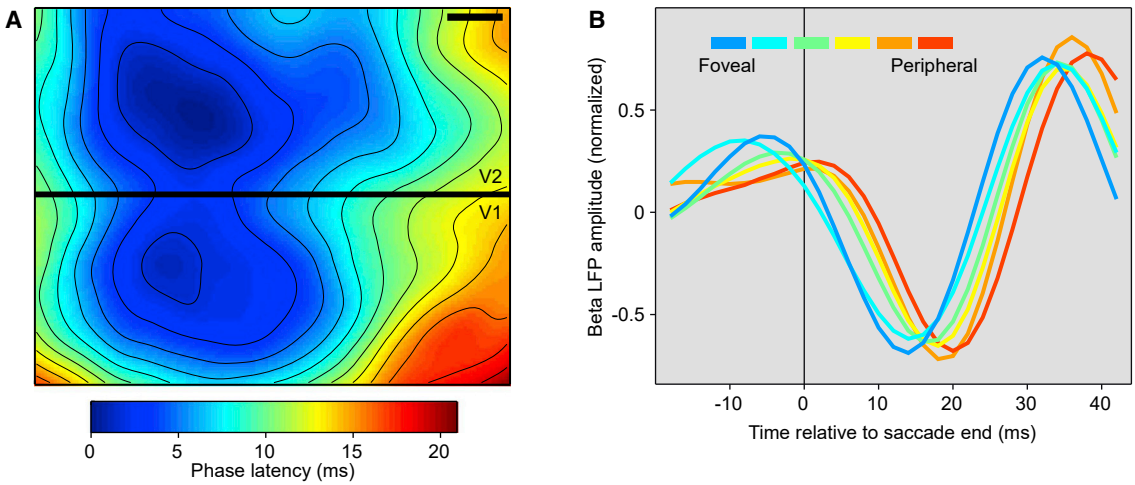

Figure 6. Evidence for waves in visual cortex traveling from stimulus location or from fovea

(A) Map of phase latencies, of voltage-sensitive dye signal, at the border between awake macaque areas V1 and V2 (black bar indicates 1 mm on cortical surface). A visual stimulus had been presented at a position in visual space represented approximately at the locations with minimal phase latency. After stimulus presentation, a wave propagates over both V1 and V2, with phase latencies increasing systematically with distance from the stimulus' representation. Adapted and modified from Muller et al.[47]

(B) Amplitude of beta-filtered LFP as a function of time relative to the end of a saccade. Each line represents one of six recording sites in awake macaque area V4, representing visual field locations ranging from fovea to periphery, as indicated by the color legend. Adapted and modified from Zanos et al.[48]

start at the fovea and travel into periphery, or they might start at an attended peripheral location or at a salient stimulus. Indeed, traveling waves in the LFP (filtered 5–40 Hz) of marmoset area MT enhance neuronal excitability and psychophysical sensitivity in a detection task,[49] consistent with attentional scans.

The last paragraphs provided evidence (1) that attentional performance benefits at the cued and the uncued location on the same stimulus have a systematic delay, (2) that a short visual stimulus triggers a traveling wave propagating from the cortical representation of the stimulus, and (3) that a saccade is triggering a similar traveling wave propagating from the cortical representation of the fovea. These three observations might well be reflecting the same underlying mechanism, because their observed or inferred traveling speeds are in a similar range. The post-saccadic traveling waves in area V4 had a mean propagation speed of 31 cm/s with a standard deviation of 8 cm/s.[48] The post-stimulation traveling waves in area V1 had a median propagation speed of 57 cm/s with a median absolute deviation of 18 cm/s.[47] In the psychophysics study, the propagation speed of putative traveling waves in areas V1 and V4 underlying the delay between attentional performance benefits can only be estimated (partly based on Figure 8 of Brewer et al.[50]), which results in propagation speeds of ~40 cm/s. Thus, the observed or inferred propagation speeds in these three studies are within less than a factor of two of each other, and close to the speed of propagation of neuronal signals along lateral connections.[51–54]

RHYTHMIC SCANNING IN THE HIPPOCAMPUS

There is an intriguing similarity between these observations in the visual system and observations in the hippocampus. The hippocampus shows prominent theta oscillations, which might be seen as segmenting information by internal attention,[28,55] similar to the way saccades segment visual information by external attention. The hippocampus is positioned on top of the hierarchy of visual areas.[56] As high-level visual areas feed into the hippocampus, and as they predominantly represent attended sensory inputs, attention likely also plays an important role in determining the momentary representation in the hippocampus. The hippocampus has been studied particularly well in rodents with regard to the representation of space. Seminal work has demonstrated hippocampal neurons that show enhanced firing rates when an animal is in a particular place in the environment, lending those cells the name place cells and their firing fields the name place fields.[57]

A recent study recorded pairs of hippocampal place cells, while rats were running on an arm of a maze that brought them to a bifurcation.[58] At the bifurcation, rats needed to run into the left arm or the right arm on alternate trials in order to obtain reward. The place fields of the two simultaneously recorded neurons extended from the bifurcation point into the left arm for cell 1 and into the right arm for cell 2 (Figure 7A). When the rat approached the bifurcation point, before entering one of the choice arms, the two place cells fired on alternate cycles of the hippocampal 8 Hz theta rhythm (Figures 7B and 7C). Thus, when the rat faced two simultaneously present movement options, the neuronal population in hippocampus sampled the two options in theta-rhythmic alternation. I propose that this is a form of theta-rhythmic attentional sampling because of the similarity to findings in the visual system during selective visual attention. When macaques face two simultaneously presented stimuli, the neuronal population in higher visual areas represents the momentarily attended stimulus,[40] and attention samples the two stimuli in theta-rhythmic alternation.[39,43,44,46]

The abovementioned evidence suggests that theta-rhythmic attentional sampling of spatially extended stimuli might proceed in the form of theta-rhythmic attentional scanning, starting

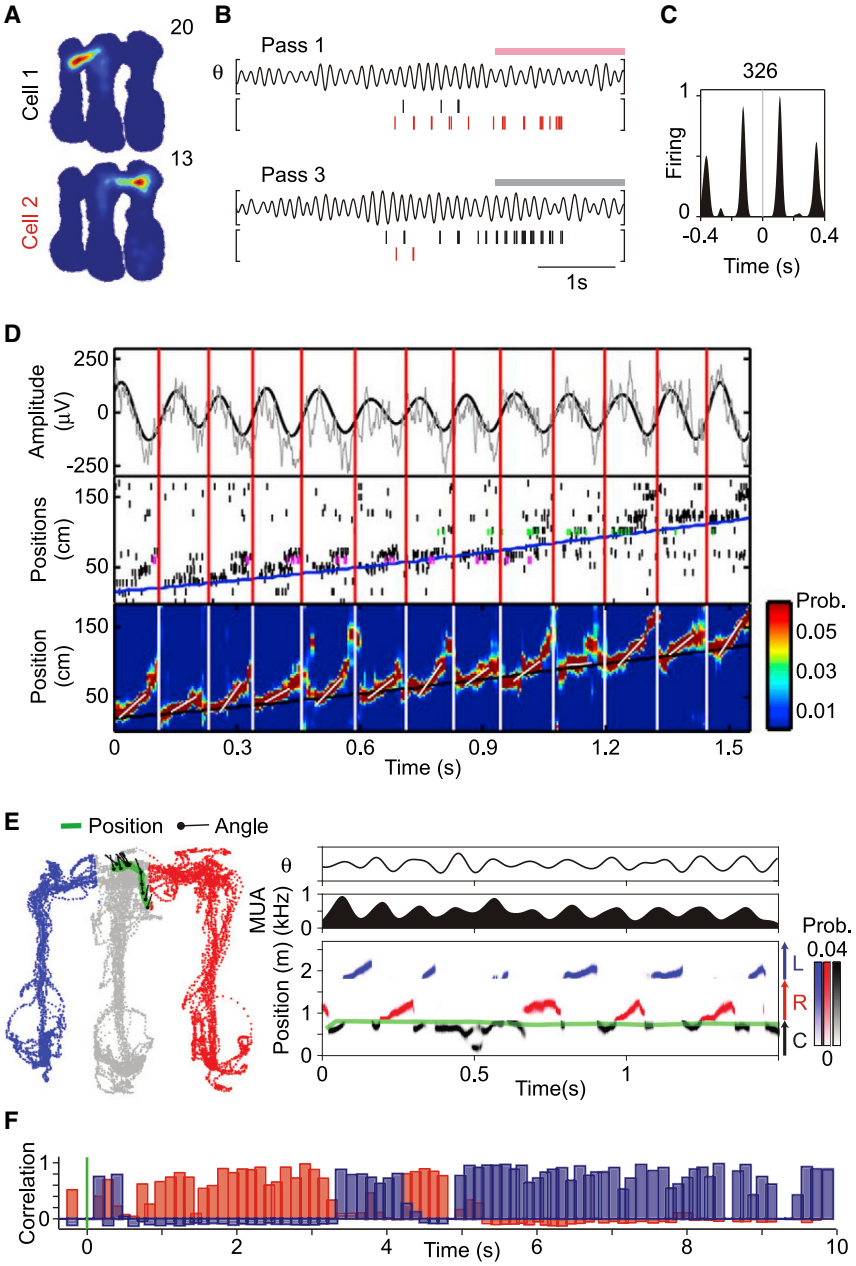

Figure 7. Theta-rhythmic scanning of space by hippocampal place cells firing in theta sequences

(A–C) Data recorded from rat hippocampus, while a rat ran in an m-shaped maze. At the end of each of the three arms, rewards could be delivered. Rats were rewarded for alternately running from the center arm into the left and right arm.

(A) Firing maps of two simultaneously recorded cells in rat hippocampus. The firing map of cell 1 extends from the center arm into the left arm, and the firing map of cell 2 extends into the right arm.

(B) Data recorded during two outbound passes from the center arm into either the right or the left arm. Pink (gray) horizontal bar marks entry into the right (left) arm. For each pass, the upper plot shows the LFP filtered in the theta band (here: 5–11 Hz), and the lower plot shows the spike times of cell 1 (black vertical lines) and cell 2 (red vertical lines).

(C) Crosscorrelogram between the spike times of cells 1 and 2.

(A)–(C) are adapted and modified from Kay et al.[58]

(D) Data recorded from rat hippocampus, while a rat ran a single pass on a linear track. Top plot: raw LFP (gray) and LFP filtered in the theta band (here: 4–12 Hz, black). Middle plot: spikes recorded simultaneously from 107 pyramidal cells in hippocampal CA1. Pyramidal cells are ordered along the y axis by their peak firing positions along the track (magenta and green indicate spikes from example neurons shown in more detail in other plots of the original paper, but not here). Bottom plot: spike-decoder-based probability estimates (color-coded) of the rat's position, referred to as theta sequence. The beginning and end of each theta sequence are indicated by vertical lines running across the three panels (red for top and middle, white for bottom plot). In the bottom plot, the superimposed short oblique white lines indicate the speed of each theta sequence. In the middle (bottom) plots, the superimposed long oblique blue (black) line indicates the running trajectory of the animal. Adapted and modified from Feng et al.[59]

(E) Same study as illustrated in (A)–(C), but now decoding theta sequences during a single pass (similar to what is done in D) while the animal is at the decision point, at the end of the center arm, with the options to run either into the left or the right arm. Left plot: position (green) and head angle (black lines) superimposed on positions visited by the rat (color-coded by maze arm: gray, center; blue, left; red, right). Right panels: top, theta-filtered LFP (here: 5–11 Hz); middle, multi-unit activity; bottom, spike-decoder-based probability estimates. Decoded position is color-coded by arm: black, center (C); red, right (R); blue, left (L). Adapted and modified from Kay et al.[58]

(F) Pearson product-moment correlations showing evolution of population vector correlations after spatial cue switching from box I to II (red, correlation with I; blue, with II; green line, cue switch). Each bar corresponds to one theta cycle. Note frequent flickers to the original representation after cue switching. Adapted and modified from Jezek et al.[60]

at the behaviorally most relevant location and scanning away from it. Intriguingly, spatial scanning has also been observed in the hippocampal place-cell population response, when it is representing spatially extended segments of the environment.[58,59,61–63] Several studies recorded sets of rat hippocampal place cells with place fields that neighbored one another along a segment of a maze. When the rat ran through that segment, the place-cell population typically represents locations within the segment (Figure 7 of Gupta et al.[61]). Yet, the representation is not always precisely at the veridical position of the animal. Rather, within each theta cycle, the representation typically starts at the position just behind the animal, scans through the actual position of the animal, and then scans forward into the future path of the animal (Figure 7D).[59] Typically, this scanning ahead extends until the next behaviorally relevant location in the maze.[61,63] I propose that this is a form of theta-rhythmic attentional scanning, that is, a version of the abovementioned theta-rhythmic attentional

sampling, which occurs when the represented item, here a maze segment, is extended.

As this scanning entails a systematic sequence of place-cell firing within the theta cycle, it is often referred to as a theta sequence. Note that the presence of theta sequences is in principle predicted by the phenomenon of theta-phase precession. Theta-phase precession is the systematic advance of place-cell firing relative to the theta cycle, as the rat runs through the respective place fields[64]: when the rat enters a place field, the respective place cell's firing rate increases, and spikes occur preferentially near the end of the theta cycle; as the rat advances toward the center of the place fields, the firing rate reaches its peak, and spiking advances toward the middle of the theta cycle; as the rat leaves the place field, even though firing rate declines, spiking typically advances further toward the start of the theta cycle. Thereby, at any position along the rat's path, the theta cycle will start with spikes from place cells whose place fields the rat is just leaving, it will proceed with spikes from place cells whose place fields are close to the rat's current position, and it will end with spikes from place cells whose place fields the rat is just entering. Thus, theta-phase precession and theta sequences are likely related phenomena. Nevertheless, theta sequences entail more neuronal coordination than predicted by the independent theta-phase precession of separate place cells,[65] probably mediated by some form of rapid learning.[59] Note that an interpretation of the theta sequence as an attentional scan might conceptually explain why theta-phase precession does not reverse when the animal leaves the place field. When the animal leaves a place field, firing rates decline, most likely because excitatory drive declines. Declining excitatory drive could in principle shift spiking to later theta phases with declining hippocampal inhibition. However, despite declining excitatory drive, spikes of place cells, whose place fields are just left, occur at early theta phases. If theta-phase precession would revert, the representation in the late theta cycle would be confused, containing both past and future locations. Rather, the data suggest that the momentary hippocampal place-cell population representation is internally coherent, scanning from the recent past into the near future. This is consistent with an undivided attentional spotlight scanning from the recent past, through the present, into the near future. Theta-phase precession is also present in human hippocampus and the entorhinal cortex during spatial navigation and in human frontal cortex while seeking specific goals.[66] Note that hippocampal theta is readily observed in the absence of sensory attention, e.g., during REM sleep, suggesting that theta assists multiple cognitive processes.

The last paragraphs have shown that the hippocampal place-cell population represents two competing options in theta-rhythmic alternation, and this representation can unfold as a theta sequence that scans the currently occupied segment of the environment in the direction of the animal's own movement. Thereby, when a rat is approaching a bifurcation, theta sequences should scan down the two alternative choice arms in theta-rhythmic alternation, and this has indeed been found (Figure 7E).[58] Importantly, these alternating scans into the two possible choice arms were not due to respective movements of the head and could occur while the rat was running at high speed toward the choice point. Thereby, these scans do not merely represent current sensory input, but reflect possible futures,[58] recalled from short-term memory (STM). Thus, these findings suggest that two items held simultaneously in STM, here the two possible choice arms, are represented in hippocampus on separate theta cycles. Note that hippocampal assemblies can scan far into the future, and thereby predict upcoming behavior, even when a rat is running in a stationary wheel,[67] suggesting that the hippocampus generally is a sequence generator.[68]

The conclusion that two items in STM are represented on separate hippocampal theta cycles is also supported by another study showing nicely how hippocampal place-cell representations of the recent past can be interspersed in individual theta cycles, in-between theta cycles in which hippocampal place cells represented the present sensory environment. A set of simultaneously recorded place cells typically shows a characteristic set of place fields in a given environment and an independent set of place fields in a different environment. In a highly original study, two different environments were created by two very different sets of LED lights in the floor and the walls of a test box.[60] Rats were first exposed to either one or the other LED-defined environment in clearly separated sessions, and sets of about 30 simultaneously recorded place cells showed independent distributions of firing in the two environments. Subsequently, rats were first placed into one environment for approximately 1 min, and then the LED lights were suddenly switched to essentially teleport the animals into the other environment. After such teleportation events, for a period of about 10 s, the hippocampal population representation was bistable, expressing either the past or the present environment. Crucially, the representation of a given environment was contained within a cycle of the hippocampal theta rhythm (Figure 7F). The representation could switch from one to the other environment between adjacent theta cycles. Yet, within a given theta cycle, the hippocampal neuronal population represented either one or the other environment and avoided mixtures. This is consistent with a theta-rhythmic formation of neuronal population attractor states.[60] It likely involves the dynamic reconfiguration of hippocampal interneuron circuits.[69] As the teleportation had switched sensory input to the new environment, the hippocampal representation of the past environment reflected STM.

PREVIOUS HYPOTHESES ABOUT THETA- (OR ALPHA-) NESTED GAMMA IN HIPPOCAMPUS AND VISUAL CORTEX

A previous modeling study proposed that each theta cycle contains the representations of approximately seven STM items, with each item represented in a gamma subcycle.[70] This hypothesis has been expanded to apply generally to neuronal coding and has been referred to as the "theta-gamma neural code[71]," or TGNC (hypothesis). Similarly, for the processing of multiple simultaneously present visual stimuli, it was proposed that the two to three most salient of those stimuli are all represented within each cycle of the alpha rhythm (~8–12 Hz), with each item represented in a gamma subcycle (Figure 8A).[72] I refer to this as the "alpha-gamma neural code," or AGNC (hypothesis). While these proposals attribute similar roles to theta and alpha, those rhythms actually show largely opposite relations to attention and sensory

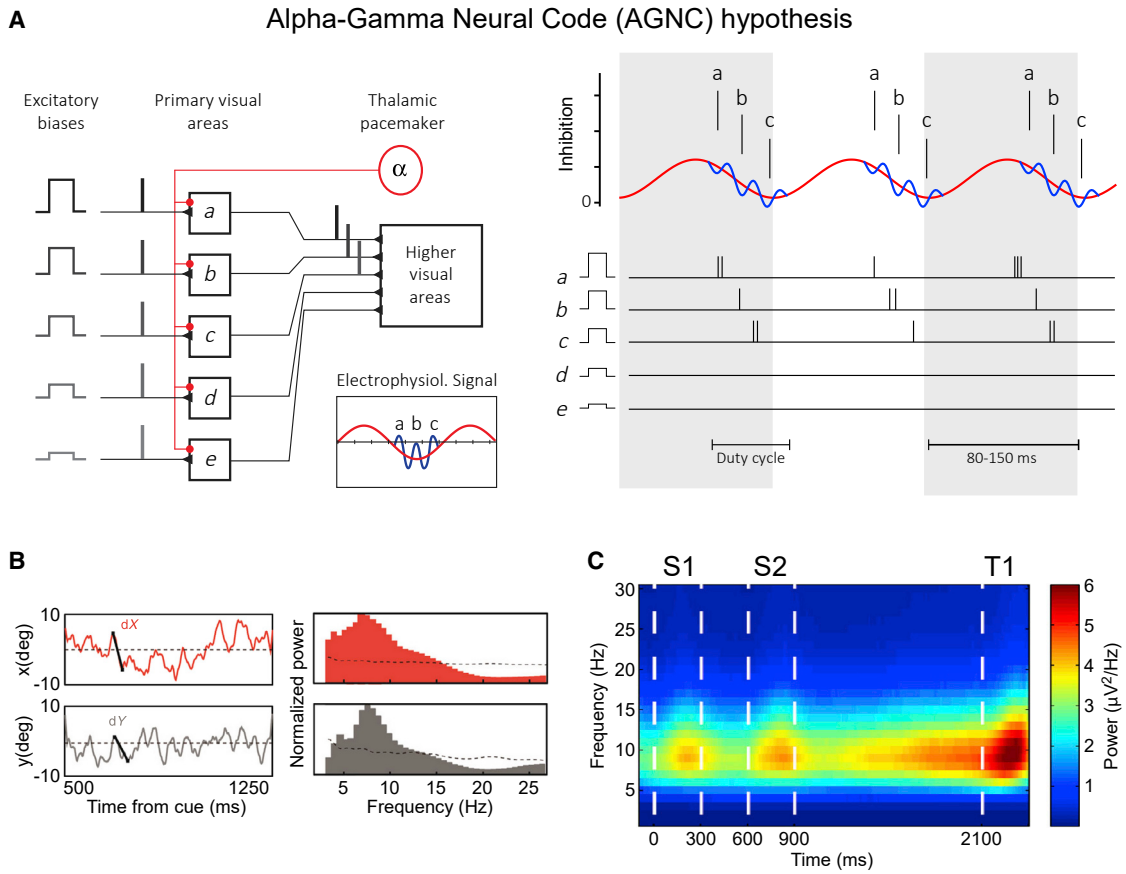

Figure 8. Alpha-gamma neural code (AGNC) hypothesis; theta rhythm in primate frontal cortex during attention and working memory

(A) Alpha-gamma neural code (AGNC) hypothesis, adapted and modified from Jensen et al.[72]: five stimuli have neuronal representations with decreasing levels of excitability, decreasing from a to e, which interact with an inhibitory oscillatory alpha drive (8–13 Hz). As a result, representations discharge in sequence a-b-c, and the less excited representations d and e, are prevented from discharge. The discharging representations are kept apart in time by fast recurrent inhibition from an interneuronal network.

(B) Left plots: x- and y-position of the attentional spotlight, decoded from multiple simultaneous recordings in macaque frontal eye field (FEF), as a function of time from attentional cue onset in one exemplary trial. Right plots: corresponding power spectra, showing peaks in the theta-frequency range. Adapted and modified from Gaillard et al.[78]

(C) Difference between spectrograms of the envelopes of the LFP gamma-band (45–100 Hz) oscillations in gamma-modulated versus non-modulated recording sites. Recordings were performed in PFC of monkeys performing a working memory task. During the task, two samples (indicated here as S1 and S2) are shown and are kept in working memory until they can be compared with the test (indicated here as T1). Adapted and modified from Lundqvist et al.[79]

stimulation: Theta is prominent during attentional exploration or working memory,[64,73,74] whereas alpha is reduced by attentional engagement or sensory stimulation.[75–77]

TGNC and RAS differ fundamentally in how theta and gamma subserve functions. TGNC proposes that segmentation is achieved by limiting the representation of a given item to a single gamma subcycle per theta cycle; attention is multiplexed across those items by processing them sequentially within each theta cycle. RAS proposes that segmentation is achieved by limiting the representation of a given item to a single theta cycle; attention is multiplexed across items by processing them sequentially within subsequent theta cycles; within each theta cycle, gamma binds and segments representations of different items in lower areas, and routes the representation of the attentionally selected item to higher areas.

An elegant computational study[80] provided a network of spiking neurons implementing both TGNC, referred to as LJ-multiplexing (Lisman Jensen), and RAS, referred to as F-multiplexing (Fries). The study demonstrated that TGNC and RAS are both plausible, and that small changes to the model switch it from one to the other scenario. In the following, I will review the relevant empirical evidence and argue that it favors the RAS hypothesis.

The AGNC hypothesis is concerned with a scenario in which multiple visual stimuli are simultaneously present (Figure 8B). AGNC predicts for primary visual cortex that a given neuron is active in one gamma subcycle per alpha cycle; the autocorrelation should show alpha-rhythmic reoccurrence of narrow gamma peaks. However, empirical autocorrelations typically show gamma modulation.[81,82] AGNC predicts further for primary visual cortex (1) that neurons representing the same stimulus fire in the same gamma subcycle of alpha, and their cross-correlation should show alpha-rhythmically reoccurring narrow gamma peaks with approximately zero time lag between the two cells

and (2) that neurons representing different stimuli fire on neighboring but separate gamma subcycles of alpha, and their cross-correlation should show alpha-rhythmically reoccurring narrow gamma peaks, with a time lag between the two cells corresponding to a small integer multiple of the gamma cycle length. However, empirical cross-correlations for neurons representing the same stimulus typically show gamma-rhythmic modulations with small or no time lag, and cross-correlations for neurons representing different stimuli typically show no significant modulation at all.[83,84] AGNC predicts for higher visual areas that a given neuron represents two to three stimuli sequentially within each alpha cycle, with each stimulus representation lasting for approximately one gamma cycle. By contrast, neurons in high-level visual areas represent different simultaneously presented stimuli on separate theta cycles.[43,85]

TGNC predicts that a given place cell should be active in only one gamma subcycle per theta cycle, and the autocorrelation should show narrow gamma peaks separated by theta-cycle-long periods of low firing rates. However, empirical autocorrelations typically show theta-rhythmic modulations, with spikes either occurring on each theta cycle (see e.g., Figure 9 of O'Keefe and Recce[64]) or on each second theta cycle (see e.g., Figure 3 of Kay et al.[58]). TGNC also predicts that place cells with neighboring but non-overlapping place fields fire on neighboring but separate gamma subcycles of the same theta cycle, and their cross-correlation should show narrow gamma peaks with a time lag between the two cells that corresponds to a small integer multiple of the gamma-cycle length. However, empirical cross-correlations typically show theta-rhythmic modulations with smoothly varying time lags (see e.g., Figure 1 of Dragoi and Buzsáki[65]). Note that the sensitivity of cross-correlations to reveal peaks at higher frequencies is limited by the number of spikes used for the calculation of the cross-correlations. Yet, cross-correlations between hippocampal spike recordings can reveal theta and no gamma, even when based on thousands of spikes (e.g., Figures 3 and S1 of Kay et al.[58]). By contrast, cross-correlations between visual cortical spike recordings can reveal gamma rhythmicity even for spike numbers in the range of few tens to few hundreds, recorded on single trials (e.g., Figures 1, 2, 3, 7, 10, and 12 of Livingstone[86]; and Figure 5B of Maldonado et al.[87]).

All the mentioned empirical evidence, which is in contradiction to the TGNC or AGNC hypothesis, is consistent with the RAS hypothesis.

One empirical observation that has been put forth to support TGNC is the phenomenon of theta sequences, the sequential firing of place cells in the theta cycle, according to the spatial position of their place fields along an animal's path. TGNC regards the positions corresponding to those place fields as separate items, each represented by an ensemble of place cells that has highly overlapping place fields and that spikes in the same gamma subcycle of a given theta cycle. TGNC proposes that each theta cycle contains approximately seven gamma subcycles, and it thereby proposes that the space scanned by a theta sequence is discretized into seven positions. However, the space in between those seven positions is almost certainly also covered by the place fields of some place cells, and it is not clear from the TGNC hypothesis when those place cells should spike. The evidence presented above suggests that the hippocampal place cell representation discretizes space in a different way, namely, such that a represented item corresponds to a behaviorally relevant segment of the environment. Such a segment might, for example, be a part of a maze that leads from a bifurcation point to a feeding point.[61]

RHYTHMIC SCANNING IN PREFRONTAL CORTEX (PFC)

Control over the deployment of selective attention is executed by the PFC. In particular, spatially selective attention is controlled by a part of the PFC called the frontal eye field (FEF).[88] One study in macaque monkeys recorded simultaneously from 24 sites in each of the two FEFs of the two hemispheres.[78] The animals foveated a central fixation point, while four peripheral locations, one in each visual quadrant, were indicated by placeholders. One of those placeholders was cued. During the trial, the uncued placeholders could undergo changes that needed to be ignored, whereas a change at the cued placeholder needed to be reported to obtain reward. Trials with attention directed to the different quadrants can be used to train a decoder of the neuronal data, which can subsequently be applied to short analysis windows sliding over the data recorded in single trials. Intriguingly, the decoded momentary position of attention was not always at the cued location but rather deviated from that location with an 8 Hz rhythmicity (Figure 8B). Note that the smooth movement of the decoded attentional spotlight suggests that attention can move continuously across visual field representations rather than necessarily jumping between locations. Jumps might be performed at theta-rhythmic resets, and smooth movements or scans within a theta cycle, as also suggested by the Fiebelkorn et al.[46] study discussed above.

Another study also used recordings of neuronal activity from FEF to infer the likely momentary location of attention during a visual search task.[89] In this task, macaques foveated a fixation point and were first presented with a sample stimulus and after a delay period with a search array with four stimuli, each in one of the visual quadrants. One of those stimuli was identical to the sample, and the animal needed to saccade to that target to obtain a reward. Saccades were preceded by 50 ms of enhanced activity in neurons with receptive fields in the target quadrant. Between 50 and 100 ms before the saccade, there was enhanced activity in neurons with receptive fields in the quadrant counterclockwise to the target. At an even earlier period, around 200 ms before the saccade, there was enhanced activity in neurons with receptive fields opposite to the target. This pattern of results is consistent with serial shifts of attention through the items in a clockwise direction, requiring $\sim$40 ms per stimulus, which is supported by relationships between the neuronal and behavioral data and the 25 Hz, beta-band component of the LFP.[89] Note that this pattern of results is also consistent with a single attentional scan through the items, with each item processed in a beta cycle and all items together being scanned within the time span corresponding to a theta cycle.

Next to attention, PFC also supports another central cognitive function, STM, relating to the ability to keep and use information about a sensory stimulus when that stimulus is not physically present. STM has been linked to neuronal rhythms, primarily

for two reasons: neuronal rhythms can help keeping a neuronal representation active, and they might explain the limited capacity of STM. In human subjects, visual STM capacity is limited to four features or four feature conjunctions, i.e., four integrated visual objects,[90] and verbal STM capacity is limited to 7 ± 2 items.[91] Explaining this verbal STM capacity limit of 7 ± 2 items has been the central aim of the TGNC hypothesis discussed above. Yet, also more recent models of STM centrally involve oscillations. One of these models implements STM items as short-lived attractor states: an attractor network model with biologically plausible synaptic plasticity can provide STM by cyclic reactivation of up to six items, with reactivation occurring at theta, and each reactivation associated with gamma.[92] Thus, contrary to the TGNC hypothesis, each theta cycle contains not all memorized items, but merely one item, and within the theta cycle, the represented item is not coded in a single gamma cycle but in several gamma cycles. This model has received strong and direct support from recordings of PFC in macaque monkeys performing an STM task.[79] These recordings revealed that gamma occurred in bursts, accompanying encoding and reactivation of sensory information, specifically at recording sites representing the to-be-remembered items. When gamma at those sites is compared with other sites, and the temporal envelope of gamma is analyzed for modulation by lower frequencies, this reveals a prominent modulation of the gamma envelope by a theta rhythm (Figure 8C),[79] even though the autocorrelation of gamma bursts did not provide clear evidence for periodicity.

If STM holds multiple items, they might be linked into a chunk, and this chunk might be theta-rhythmically scanned. Indeed, a study using intracranial electrode recordings in human epilepsy patients reported evidence consistent with this. Participants were shown sequences of three letters, which they kept in STM during a maintenance period, to later decide about whether or not a fourth letter had been part of the prior sequence.[93] Some of the recording sites showed gamma-band responses to letter presentation that differed across the three letters. During STM maintenance, these letter-selective sites showed theta-phase-dependent gamma-band responses reflecting the memorized letter sequence: within each theta cycle, the average gamma-band power was initially highest for sites responsive to the first letter, then for sites responsive to the second letter, and finally for sites responsive to the third letter. Note that these results are also broadly consistent with the TGNC hypothesis.[93] Yet, the TGNC hypothesis would predict that STM for three letters would lead to three gamma cycles per theta cycle, with the first gamma cycle containing the representation of the first letter, and so on. This evidence was not reported. Therefore, an alternative and parsimonious interpretation is that the observed sequence reflects a theta-rhythmic attentional scan across an STM chunk composed of the three letters.

SUMMARY AND OUTLOOK

In summary, observations across several brain areas, including V1, V2, V4, IT, hippocampus, and PFC, and across several cognitive functions, including early visual processing, object recognition, selective attention, spatial navigation, and STM, suggest a shared RAS scenario: when multiple items (or options) are present simultaneously, each item is represented in a gamma-synchronized neuronal group, and different items are fully processed and represented across areas in separate theta cycles. When items are extended, their representations are theta-rhythmically scanned by a traveling wave.

In the visual system, when the input contains multiple items simultaneously, their corresponding gamma-synchronized neuronal ensembles coexist in V1, and one item is attentionally selected per theta cycle for entrainment of and corresponding routing to higher visual areas. In hippocampus, when an animal is uncertain about being located in one of two possible environments, each environment is represented in a separate theta cycle, and when spatial navigation could go into multiple directions, each direction is represented in a separate theta cycle; similar to the visual cortex, hippocampal neuronal representations also entail gamma synchronization.[1,94] In PFC, when STM holds multiple items, each item is represented by an attractor state entailing gamma synchronization, and the different items are represented in different theta cycles. Yet, RAS most likely does not explain all occurrences of theta and/or gamma, as suggested by theta during REM sleep. Further research is needed to investigate whether RAS applies to theta in the auditory system[95] or frontal theta during cognitive control.[96]

The representation in a theta cycle can be organized as a traveling wave. In the visual system, saccades occur theta rhythmically and cause theta-rhythmic visual stimulus onsets; saccades and stimulus onsets trigger waves traveling across visual cortex and thereby across its representational space. During fixation, after an attentional cue at one position of an extended visual object, detection performance fluctuates in a way consistent with a theta-rhythmic attentional scanning of the object. In hippocampus, during navigation on a linear track, the decoded spatial representation theta-rhythmically scans the space, often starting at the current or just-visited location and scanning across the upcoming locations; during decision-making at a point where an animal can navigate into one of two directions, the decoded spatial representation theta-rhythmically alternates between scanning into the two directions. In PFC, when multiple simple items are repeatedly co-occurring, they might be linked into a chunk, which is then theta-rhythmically scanned. The evidence for scanning is mostly related to representational items that are extended, like extended visual stimuli[46] or extended segments of the environment.[58,59,61–63] Yet, any item is extended to some degree, such that its sampling might always proceed in the form of scanning. As this scanning corresponds to traveling waves, it might in fact be a general feature of the cortex. When the visual cortex is activated by a small stimulus, a traveling wave propagates through substantial portions of the surrounding map of visual space.[47] Even the spontaneous spiking of single neurons is followed by a wave traveling across the cortex, away from the neuron.[97]

RAS predicts some degree of theta coherence between brain areas, but the respective evidence is still limited. In human epilepsy patients, theta coherence between intracranial EEG recordings declines with distance and is largely absent beyond 20 mm.[98] Thus, human frontal midline theta, likely involved in RAS,[37] might be unrelated to hippocampal theta.[99] Yet, in rodents, theta coherence has been reported between

hippocampus and the frontal[100,101] as well as visual[102] cortex. Also in non-human primates, the available evidence suggests dynamic coordination of theta across areas: the decoded attentional spotlight in FEF theta-rhythmically scans space;[78] and FEF determines the attentional focus in V4.[88] During an attention task, V4 and FEF show long-range coupling at theta frequencies, yet attention effects occur mainly at gamma frequencies.[103] Theta in V4 and V1 is at least partially coherent.[2,25] Also, V4 and PFC can show theta coherence during the memory period of an STM task.[73] The non-human primate hippocampus shows theta rhythmicity during visual exploration, with each saccade resetting theta phase.[33] Saccades, and even microsaccades, reset the phase of ongoing rhythms, and particularly lower-frequency components like theta, also in V1 and V4.[104–106] Thus, saccades likely coordinate (theta) phase resets across the visual system and hippocampus.

Within those coordinated theta cycles, theta-rhythmic attentional scanning might also be coordinated between the visual cortex and hippocampus. However, as this scanning might be organized in the representational spaces of the respective areas, it might as well be independent between areas. Also, two representational spaces embedded in the same area, like the hippocampal representations for a rat's spatial location and its head direction, can both be theta-rhythmically scanned at the same time.[58] Investigating these dynamics will require simultaneous dense and space-covering recordings from several areas. Such recordings have become possible,[107–109] and they will be essential for a better understanding of rhythmic attentional scanning.

ACKNOWLEDGMENTS

This work was supported by DFG (FOR 1847 FR2557/2-1, FR2557/5-1-CORNET, FR2557/7-1-DualStreams), EU (HEALTH-F2-2008-200728-BrainSynch, FP7-604102-HBP), a European Young Investigator Award, and the National Institutes of Health (1U54MH091657-WU-Minn-Consortium-HCP).

DECLARATION OF INTERESTS

P.F. has a patent on thin-film electrodes and is a beneficiary of a respective license contract with Blackrock Microsystems (Salt Lake City, UT, USA). P.F. is a member of the Advisory Board of CorTec (Freiburg, Germany).

REFERENCES

1. Bragin, A., Jandó, G., Nádasdy, Z., Hetke, J., Wise, K., and Buzsáki, G. (1995). Gamma (40–100 Hz) oscillation in the hippocampus of the behaving rat. J. Neurosci. *15*, 47–60.

2. Spyropoulos, G., Bosman, C.A., and Fries, P. (2018). A theta rhythm in macaque visual cortex and its attentional modulation. Proc. Natl. Acad. Sci. USA *115*, E5614–E5623. https://doi.org/10.1073/pnas.1719433115.

3. Colgin, L.L., Denninger, T., Fyhn, M., Hafting, T., Bonnevie, T., Jensen, O., Moser, M.B., and Moser, E.I. (2009). Frequency of gamma oscillations routes flow of information in the hippocampus. Nature *462*, 353–357. https://doi.org/10.1038/nature08573.

4. Canolty, R.T., Edwards, E., Dalal, S.S., Soltani, M., Nagarajan, S.S., Kirsch, H.E., Berger, M.S., Barbaro, N.M., and Knight, R.T. (2006). High gamma power is phase-locked to theta oscillations in human neocortex. Science *313*, 1626–1628. https://doi.org/10.1126/science.1128115.

5. Posner, M.I., Snyder, C.R., and Davidson, B.J. (1980). Attention and the detection of signals. J. Exp. Psychol. *109*, 160–174.

6. Anderson, B. (2011). There is no such thing as attention. Front. Psychol. *2*, 246. https://doi.org/10.3389/fpsyg.2011.00246.

7. James, W. (1890). The Principles of Psychology (Henry Holt and Company).

8. Buzsáki, G. (2019). The Brain from inside Out (Oxford University Press).

9. Salin, P.A., Girard, P., Kennedy, H., and Bullier, J. (1992). Visuotopic organization of corticocortical connections in the visual system of the cat. J. Comp. Neurol. *320*, 415–434. https://doi.org/10.1002/cne.903200402.

10. Lund, J.S., Angelucci, A., and Bressloff, P.C. (2003). Anatomical substrates for functional columns in macaque monkey primary visual cortex. Cereb. Cortex *13*, 15–24. https://doi.org/10.1093/cercor/13.1.15.

11. Desimone, R., and Duncan, J. (1995). Neural mechanisms of selective visual attention. Annu. Rev. Neurosci. *18*, 193–222. https://doi.org/10.1146/annurev.ne.18.030195.001205.

12. Reynolds, J.H., Chelazzi, L., and Desimone, R. (1999). Competitive mechanisms subserve attention in macaque areas V2 and V4. J. Neurosci. *19*, 1736–1753.

13. Reynolds, J.H., and Heeger, D.J. (2009). The normalization model of attention. Neuron *61*, 168–185. https://doi.org/10.1016/j.neuron.2009.01.002.

14. Andersen, R.A., Essick, G.K., and Siegel, R.M. (1985). Encoding of spatial location by posterior parietal neurons. Science *230*, 456–458. https://doi.org/10.1126/science.4048942.

15. Azouz, R., and Gray, C.M. (2003). Adaptive coincidence detection and dynamic gain control in visual cortical neurons in vivo. Neuron *37*, 513–523.

16. Salinas, E., and Sejnowski, T.J. (2001). Correlated neuronal activity and the flow of neural information. Nat. Rev. Neurosci. *2*, 539–550. https://doi.org/10.1038/35086012.

17. Fries, P., Reynolds, J.H., Rorie, A.E., and Desimone, R. (2001). Modulation of oscillatory neuronal synchronization by selective visual attention. Science *291*, 1560–1563. https://doi.org/10.1126/science.1055465.

18. Bichot, N.P., Rossi, A.F., and Desimone, R. (2005). Parallel and serial neural mechanisms for visual search in macaque area V4. Science *308*, 529–534. https://doi.org/10.1126/science.1109676.

19. Taylor, K., Mandon, S., Freiwald, W.A., and Kreiter, A.K. (2005). Coherent oscillatory activity in monkey area V4 predicts successful allocation of attention. Cereb. Cortex *15*, 1424–1437. https://doi.org/10.1093/cercor/bhi023.

20. Womelsdorf, T., Fries, P., Mitra, P.P., and Desimone, R. (2006). Gamma-band synchronization in visual cortex predicts speed of change detection. Nature *439*, 733–736. https://doi.org/10.1038/nature04258.

21. Fries, P. (2005). A mechanism for cognitive dynamics: neuronal communication through neuronal coherence. Trends Cogn. Sci. *9*, 474–480. https://doi.org/10.1016/j.tics.2005.08.011.

22. Fries, P. (2015). Rhythms for cognition: communication through coherence. Neuron *88*, 220–235. https://doi.org/10.1016/j.neuron.2015.09.034.

23. Börgers, C., and Kopell, N.J. (2008). Gamma oscillations and stimulus selection. Neural Comput. *20*, 383–414. https://doi.org/10.1162/neco.2007.07-06-289.

24. Lewis, C.M., Ni, J., Wunderle, T., Jendritza, P., Lazar, A., Diester, I., and Fries, P. (2021). Cortical gamma-band resonance preferentially transmits coherent input. Cell Rep. *35*, 109083. https://doi.org/10.1016/j.celrep.2021.109083.

25. Bosman, C.A., Schoffelen, J.M., Brunet, N., Oostenveld, R., Bastos, A.M., Womelsdorf, T., Rubehn, B., Stieglitz, T., De Weerd, P., and Fries, P. (2012). Attentional stimulus selection through selective synchronization between monkey visual areas. Neuron *75*, 875–888. https://doi.org/10.1016/j.neuron.2012.06.037.

26. Grothe, I., Neitzel, S.D., Mandon, S., and Kreiter, A.K. (2012). Switching neuronal inputs by differential modulations of gamma-band phase-coherence. J. Neurosci. *32*, 16172–16180. https://doi.org/10.1523/JNEUROSCI.0890-12.2012.

27. Rohenkohl, G., Bosman, C.A., and Fries, P. (2018). Gamma synchronization between V1 and V4 improves behavioral performance. Neuron *100*, 953–963.e3. https://doi.org/10.1016/j.neuron.2018.09.019.

28. Buzsáki, G. (2010). Neural syntax: cell assemblies, synapsembles, and readers. Neuron *68*, 362–385. https://doi.org/10.1016/j.neuron.2010.09.023.

29. Crick, F. (1984). Function of the thalamic reticular complex: the searchlight hypothesis. Proc. Natl. Acad. Sci. USA *81*, 4586–4590. https://doi.org/10.1073/pnas.81.14.4586.

30. Kirchner, H., and Thorpe, S.J. (2006). Ultra-rapid object detection with saccadic eye movements: visual processing speed revisited. Vision Res. *46*, 1762–1776. https://doi.org/10.1016/j.visres.2005.10.002.

31. Thorpe, S., Fize, D., and Marlot, C. (1996). Speed of processing in the human visual system. Nature *381*, 520–522. https://doi.org/10.1038/381520a0.

32. Senzai, Y., Fernandez-Ruiz, A., and Buzsáki, G. (2019). Layer-specific physiological features and interlaminar interactions in the primary visual cortex of the mouse. Neuron *101*, 500–513.e5. https://doi.org/10.1016/j.neuron.2018.12.009.

33. Jutras, M.J., Fries, P., and Buffalo, E.A. (2013). Oscillatory activity in the monkey hippocampus during visual exploration and memory formation. Proc. Natl. Acad. Sci. USA *110*, 13144–13149. https://doi.org/10.1073/pnas.1302351110.

34. Hafed, Z.M., and Clark, J.J. (2002). Microsaccades as an overt measure of covert attention shifts. Vision Res. *42*, 2533–2545. https://doi.org/10.1016/s0042-6989(02)00263-8.

35. Otero-Millan, J., Troncoso, X.G., Macknik, S.L., Serrano-Pedraza, I., and Martinez-Conde, S. (2008). Saccades and microsaccades during visual fixation, exploration, and search: foundations for a common saccadic generator. J. Vis. *8*, 21.1–2118. https://doi.org/10.1167/8.14.21.

36. Hogendoorn, H. (2016). Voluntary saccadic eye movements ride the attentional rhythm. J. Cogn. Neurosci. *28*, 1625–1635. https://doi.org/10.1162/jocn_a_00986.

37. Busch, N.A., Dubois, J., and VanRullen, R. (2009). The phase of ongoing EEG oscillations predicts visual perception. J. Neurosci. *29*, 7869–7876. https://doi.org/10.1523/JNEUROSCI.0113-09.2009.

38. Siegel, M., Donner, T.H., Oostenveld, R., Fries, P., and Engel, A.K. (2008). Neuronal synchronization along the dorsal visual pathway reflects the focus of spatial attention. Neuron *60*, 709–719. https://doi.org/10.1016/j.neuron.2008.09.010.

39. Landau, A.N., Schreyer, H.M., van Pelt, S., and Fries, P. (2015). Distributed attention is implemented through theta-rhythmic gamma modulation. Curr. Biol. *25*, 2332–2337. https://doi.org/10.1016/j.cub.2015.07.048.

40. Moran, J., and Desimone, R. (1985). Selective attention gates visual processing in the extrastriate cortex. Science *229*, 782–784.

41. Zhang, Y., Meyers, E.M., Bichot, N.P., Serre, T., Poggio, T.A., and Desimone, R. (2011). Object decoding with attention in inferior temporal cortex. Proc. Natl. Acad. Sci. USA *108*, 8850–8855. https://doi.org/10.1073/pnas.1100999108.

42. Egeth, H.E., and Yantis, S. (1997). Visual attention: control, representation, and time course. Annu. Rev. Psychol. *48*, 269–297. https://doi.org/10.1146/annurev.psych.48.1.269.

43. Rollenhagen, J.E., and Olson, C.R. (2005). Low-frequency oscillations arising from competitive interactions between visual stimuli in macaque inferotemporal cortex. J. Neurophysiol. *94*, 3368–3387. https://doi.org/10.1152/jn.00158.2005.

44. Landau, A.N., and Fries, P. (2012). Attention samples stimuli rhythmically. Curr. Biol. *22*, 1000–1004. https://doi.org/10.1016/j.cub.2012.03.054.

45. Holcombe, A.O., and Chen, W.Y. (2013). Splitting attention reduces temporal resolution from 7 Hz for tracking one object to <3 Hz when tracking three. J. Vis. *13*, 12. https://doi.org/10.1167/13.1.12.

46. Fiebelkorn, I.C., Saalmann, Y.B., and Kastner, S. (2013). Rhythmic sampling within and between objects despite sustained attention at a cued location. Curr. Biol. *23*, 2553–2558. https://doi.org/10.1016/j.cub.2013.10.063.

47. Muller, L., Reynaud, A., Chavane, F., and Destexhe, A. (2014). The stimulus-evoked population response in visual cortex of awake monkey is a propagating wave. Nat. Commun. *5*, 3675. https://doi.org/10.1038/ncomms4675.

48. Zanos, T.P., Mineault, P.J., Nasiotis, K.T., Guitton, D., and Pack, C.C. (2015). A sensorimotor role for traveling waves in primate visual cortex. Neuron *85*, 615–627. https://doi.org/10.1016/j.neuron.2014.12.043.

49. Davis, Z.W., Muller, L., Martinez-Trujillo, J., Sejnowski, T., and Reynolds, J.H. (2020). Spontaneous travelling cortical waves gate perception in behaving primates. Nature *587*, 432–436. https://doi.org/10.1038/s41586-020-2802-y.

50. Brewer, A.A., Press, W.A., Logothetis, N.K., and Wandell, B.A. (2002). Visual areas in macaque cortex measured using functional magnetic resonance imaging. J. Neurosci. *22*, 10416–10426.

51. Benucci, A., Frazor, R.A., and Carandini, M. (2007). Standing waves and traveling waves distinguish two circuits in visual cortex. Neuron *55*, 103–117. https://doi.org/10.1016/j.neuron.2007.06.017.

52. Nauhaus, I., Busse, L., Carandini, M., and Ringach, D.L. (2009). Stimulus contrast modulates functional connectivity in visual cortex. Nat. Neurosci. *12*, 70–76. https://doi.org/10.1038/nn.2232.

53. Girard, P., Hupé, J.M., and Bullier, J. (2001). Feedforward and feedback connections between areas V1 and V2 of the monkey have similar rapid conduction velocities. J. Neurophysiol. *85*, 1328–1331. https://doi.org/10.1152/jn.2001.85.3.1328.

54. Grinvald, A., Lieke, E.E., Frostig, R.D., and Hildesheim, R. (1994). Cortical point-spread function and long-range lateral interactions revealed by real-time optical imaging of macaque monkey primary visual cortex. J. Neurosci. *14*, 2545–2568. https://doi.org/10.1523/JNEUROSCI.14-05-02545.1994.

55. Buzsáki, G. (2006). Rhythms of the Brain (Oxford University Press).

56. Felleman, D.J., and Van Essen, D.C. (1991). Distributed hierarchical processing in the primate cerebral cortex. Cereb. Cortex *1*, 1–47.

57. O'Keefe, J., and Dostrovsky, J. (1971). The hippocampus as a spatial map. Preliminary evidence from unit activity in the freely-moving rat. Brain Res. *34*, 171–175. https://doi.org/10.1016/0006-8993(71)90358-1.

58. Kay, K., Chung, J.E., Sosa, M., Schor, J.S., Karlsson, M.P., Larkin, M.C., Liu, D.F., and Frank, L.M. (2020). Constant sub-second cycling between representations of possible futures in the hippocampus. Cell *180*, 552–567.e25. https://doi.org/10.1016/j.cell.2020.01.014.

59. Feng, T., Silva, D., and Foster, D.J. (2015). Dissociation between the experience-dependent development of hippocampal theta sequences and single-trial phase precession. J. Neurosci. *35*, 4890–4902. https://doi.org/10.1523/JNEUROSCI.2614-14.2015.

60. Jezek, K., Henriksen, E.J., Treves, A., Moser, E.I., and Moser, M.B. (2011). Theta-paced flickering between place-cell maps in the hippocampus. Nature *478*, 246–249. https://doi.org/10.1038/nature10439.

61. Gupta, A.S., van der Meer, M.A., Touretzky, D.S., and Redish, A.D. (2012). Segmentation of spatial experience by hippocampal θ sequences. Nat. Neurosci. *15*, 1032–1039. https://doi.org/10.1038/nn.3138.

62. Johnson, A., and Redish, A.D. (2007). Neural ensembles in CA3 transiently encode paths forward of the animal at a decision point. J. Neurosci. *27*, 12176–12189. https://doi.org/10.1523/JNEUROSCI.3761-07.2007.

63. Wikenheiser, A.M., and Redish, A.D. (2015). Hippocampal theta sequences reflect current goals. Nat. Neurosci. *18*, 289–294. https://doi.org/10.1038/nn.3909.

64. O'Keefe, J., and Recce, M.L. (1993). Phase relationship between hippocampal place units and the EEG theta rhythm. Hippocampus *3*, 317–330. https://doi.org/10.1002/hipo.450030307.

65. Dragoi, G., and Buzsáki, G. (2006). Temporal encoding of place sequences by hippocampal cell assemblies. Neuron *50*, 145–157. https://doi.org/10.1016/j.neuron.2006.02.023.

66. Qasim, S.E., Fried, I., and Jacobs, J. (2021). Phase precession in the human hippocampus and entorhinal cortex. Cell *184*, 3242–3255.e10. https://doi.org/10.1016/j.cell.2021.04.017.

67. Pastalkova, E., Itskov, V., Amarasingham, A., and Buzsáki, G. (2008). Internally generated cell assembly sequences in the rat hippocampus. Science *321*, 1322–1327. https://doi.org/10.1126/science.1159775.

68. Buzsáki, G., and Tingley, D. (2018). Space and time: the hippocampus as a sequence generator. Trends Cogn. Sci. *22*, 853–869. https://doi.org/10.1016/j.tics.2018.07.006.

69. Dupret, D., O'Neill, J., and Csicsvari, J. (2013). Dynamic reconfiguration of hippocampal interneuron circuits during spatial learning. Neuron *78*, 166–180. https://doi.org/10.1016/j.neuron.2013.01.033.

70. Lisman, J.E., and Idiart, M.A. (1995). Storage of 7 +/- 2 short-term memories in oscillatory subcycles. Science *267*, 1512–1515.

71. Lisman, J.E., and Jensen, O. (2013). The θ-γ neural code. Neuron *77*, 1002–1016. https://doi.org/10.1016/j.neuron.2013.03.007.

72. Jensen, O., Gips, B., Bergmann, T.O., and Bonnefond, M. (2014). Temporal coding organized by coupled alpha and gamma oscillations prioritize visual processing. Trends Neurosci. *37*, 357–369. https://doi.org/10.1016/j.tins.2014.04.001.

73. Liebe, S., Hoerzer, G.M., Logothetis, N.K., and Rainer, G. (2012). Theta coupling between V4 and prefrontal cortex predicts visual short-term memory performance. Nat. Neurosci. *15*, 456–462. https://doi.org/10.1038/nn.3038.

74. Raghavachari, S., Kahana, M.J., Rizzuto, D.S., Caplan, J.B., Kirschen, M.P., Bourgeois, B., Madsen, J.R., and Lisman, J.E. (2001). Gating of human theta oscillations by a working memory task. J. Neurosci. *21*, 3175–3183.

75. Worden, M.S., Foxe, J.J., Wang, N., and Simpson, G.V. (2000). Anticipatory biasing of visuospatial attention indexed by retinotopically specific alpha-band electroencephalography increases over occipital cortex. J. Neurosci. *20*, RC63.

76. Fries, P., Womelsdorf, T., Oostenveld, R., and Desimone, R. (2008). The effects of visual stimulation and selective visual attention on rhythmic neuronal synchronization in macaque area V4. J. Neurosci. *28*, 4823–4835. https://doi.org/10.1523/JNEUROSCI.4499-07.2008.

77. Lakatos, P., Barczak, A., Neymotin, S.A., McGinnis, T., Ross, D., Javitt, D.C., and O'Connell, M.N. (2016). Global dynamics of selective attention and its lapses in primary auditory cortex. Nat. Neurosci. *19*, 1707–1717. https://doi.org/10.1038/nn.4386.

78. Gaillard, C., Ben Hadj Hassen, S., Di Bello, F., Bihan-Poudec, Y., VanRullen, R., and Ben Hamed, S. (2020). Prefrontal attentional saccades explore space rhythmically. Nat. Commun. *11*, 925. https://doi.org/10.1038/s41467-020-14649-7.

79. Lundqvist, M., Rose, J., Herman, P., Brincat, S.L., Buschman, T.J., and Miller, E.K. (2016). Gamma and beta bursts underlie working memory. Neuron *90*, 152–164. https://doi.org/10.1016/j.neuron.2016.02.028.

80. McLelland, D., and VanRullen, R. (2016). Theta-gamma coding meets communication-through-coherence: neuronal oscillatory multiplexing theories reconciled. PLoS Comput. Biol. *12*, e1005162. https://doi.org/10.1371/journal.pcbi.1005162.

81. Friedman-Hill, S., Maldonado, P.E., and Gray, C.M. (2000). Dynamics of striate cortical activity in the alert macaque: I. Incidence and stimulus-dependence of gamma-band neuronal oscillations. Cereb. Cortex *10*, 1105–1116.

82. Gray, C.M., and Singer, W. (1989). Stimulus-specific neuronal oscillations in orientation columns of cat visual cortex. Proc. Natl. Acad. Sci. USA *86*, 1698–1702.

83. Gray, C.M., König, P., Engel, A.K., and Singer, W. (1989). Oscillatory responses in cat visual cortex exhibit inter-columnar synchronization which reflects global stimulus properties. Nature *338*, 334–337. https://doi.org/10.1038/338334a0.

84. Freiwald, W.A., Kreiter, A.K., and Singer, W. (1995). Stimulus dependent intercolumnar synchronization of single unit responses in cat area 17. NeuroReport *6*, 2348–2352. https://doi.org/10.1097/00001756-199511270-00018.

85. Fries, P. (2009). Neuronal gamma-band synchronization as a fundamental process in cortical computation. Annu. Rev. Neurosci. *32*, 209–224. https://doi.org/10.1146/annurev.neuro.051508.135603.

86. Livingstone, M.S. (1996). Oscillatory firing and interneuronal correlations in squirrel monkey striate cortex. J. Neurophysiol. *75*, 2467–2485.

87. Maldonado, P.E., Friedman-Hill, S., and Gray, C.M. (2000). Dynamics of striate cortical activity in the alert macaque: II. Fast time scale synchronization. Cereb. Cortex *10*, 1117–1131.

88. Moore, T., and Fallah, M. (2001). Control of eye movements and spatial attention. Proc. Natl. Acad. Sci. USA *98*, 1273–1276. https://doi.org/10.1073/pnas.98.3.1273.

89. Buschman, T.J., and Miller, E.K. (2009). Serial, covert shifts of attention during visual search are reflected by the frontal eye fields and correlated with population oscillations. Neuron *63*, 386–396. https://doi.org/10.1016/j.neuron.2009.06.020.

90. Luck, S.J., and Vogel, E.K. (1997). The capacity of visual working memory for features and conjunctions. Nature *390*, 279–281. https://doi.org/10.1038/36846.

91. Miller, G.A. (1956). The magical number seven plus or minus two: some limits on our capacity for processing information. Psychol. Rev. *63*, 81–97.

92. Lundqvist, M., Herman, P., and Lansner, A. (2011). Theta and gamma power increases and alpha/beta power decreases with memory load in an attractor network model. J. Cogn. Neurosci. *23*, 3008–3020. https://doi.org/10.1162/jocn_a_00029.

93. Bahramisharif, A., Jensen, O., Jacobs, J., and Lisman, J. (2018). Serial representation of items during working memory maintenance at letter-selective cortical sites. PLoS Biol. *16*, e2003805. https://doi.org/10.1371/journal.pbio.2003805.

94. MacKay, D.J.C. (2003). Information Theory, Inference and Learning Algorithms (Cambridge University Press).

95. Giraud, A.L., and Poeppel, D. (2012). Cortical oscillations and speech processing: emerging computational principles and operations. Nat. Neurosci. *15*, 511–517. https://doi.org/10.1038/nn.3063.

96. Cavanagh, J.F., and Frank, M.J. (2014). Frontal theta as a mechanism for cognitive control. Trends Cogn. Sci. *18*, 414–421. https://doi.org/10.1016/j.tics.2014.04.012.

97. Nauhaus, I., Busse, L., Ringach, D.L., and Carandini, M. (2012). Robustness of traveling waves in ongoing activity of visual cortex. J. Neurosci. *32*, 3088–3094. https://doi.org/10.1523/JNEUROSCI.5827-11.2012.

98. Raghavachari, S., Lisman, J.E., Tully, M., Madsen, J.R., Bromfield, E.B., and Kahana, M.J. (2006). Theta oscillations in human cortex during a working-memory task: evidence for local generators. J. Neurophysiol. *95*, 1630–1638. https://doi.org/10.1152/jn.00409.2005.

99. Mitchell, D.J., McNaughton, N., Flanagan, D., and Kirk, I.J. (2008). Frontal-midline theta from the perspective of hippocampal "theta". Prog. Neurobiol. *86*, 156–185. https://doi.org/10.1016/j.pneurobio.2008.09.005.

100. Siapas, A.G., Lubenov, E.V., and Wilson, M.A. (2005). Prefrontal phase locking to hippocampal theta oscillations. Neuron *46*, 141–151. https://doi.org/10.1016/j.neuron.2005.02.028.

101. Jones, M.W., and Wilson, M.A. (2005). Theta rhythms coordinate hippocampal-prefrontal interactions in a spatial memory task. PLoS Biol. *3*, e402. https://doi.org/10.1371/journal.pbio.0030402.

102. Fournier, J., Saleem, A.B., Diamanti, E.M., Wells, M.J., Harris, K.D., and Carandini, M. (2020). Mouse visual cortex is modulated by distance traveled and by theta oscillations. Curr. Biol. *30*, 3811–3817.e6. https://doi.org/10.1016/j.cub.2020.07.006.

103. Gregoriou, G.G., Gotts, S.J., Zhou, H., and Desimone, R. (2009). High-frequency, long-range coupling between prefrontal and visual cortex during attention. Science *324*, 1207–1210. https://doi.org/10.1126/science.1171402.

104. Rajkai, C., Lakatos, P., Chen, C.M., Pincze, Z., Karmos, G., and Schroeder, C.E. (2008). Transient cortical excitation at the onset of visual fixation. Cereb. Cortex *18*, 200–209. https://doi.org/10.1093/cercor/bhm046.

105. Bosman, C.A., Womelsdorf, T., Desimone, R., and Fries, P. (2009). A microsaccadic rhythm modulates gamma-band synchronization and behavior. J. Neurosci. *29*, 9471–9480. https://doi.org/10.1523/JNEUROSCI.1193-09.2009.

106. Brunet, N., Bosman, C.A., Roberts, M., Oostenveld, R., Womelsdorf, T., De Weerd, P., and Fries, P. (2015). Visual cortical gamma-band activity during free viewing of natural images. Cereb. Cortex *25*, 918–926. https://doi.org/10.1093/cercor/bht280.

107. Luan, L., Wei, X., Zhao, Z., Siegel, J.J., Potnis, O., Tuppen, C.A., Lin, S., Kazmi, S., Fowler, R.A., Holloway, S., et al. (2017). Ultraflexible nanoelectronic probes form reliable, glial scar-free neural integration. Sci. Adv. *3*, e1601966. https://doi.org/10.1126/sciadv.1601966.

108. Berényi, A., Somogyvári, Z., Nagy, A.J., Roux, L., Long, J.D., Fujisawa, S., Stark, E., Leonardo, A., Harris, T.D., and Buzsáki, G. (2014). Large-scale, high-density (up to 512 channels) recording of local circuits in behaving animals. J. Neurophysiol. *111*, 1132–1149. https://doi.org/10.1152/jn.00785.2013.

109. Chung, J.E., Joo, H.R., Fan, J.L., Liu, D.F., Barnett, A.H., Chen, S., Geaghan-Breiner, C., Karlsson, M.P., Karlsson, M., Lee, K.Y., et al. (2019). High-density, long-lasting, and multi-region electrophysiological recordings using polymer electrode arrays. Neuron *101*, 21–31.e5. https://doi.org/10.1016/j.neuron.2018.11.002.